Fernández-Álvarez, María; Velasco, Francisco; Bautista, Asunción; Galiana, Beatriz (2020). Functionalizing organic powder coatings with nanoparticles through ball milling for wear applications. *Applied Surface Science,* 513, 145834.

DOI: https://doi.org/10.1016/j.apsusc.2020.145834

Functionalizing organic powder coatings with nanoparticles through ball milling for wear applications

María Fernández-Álvarez [a,*], Francisco Velasco [a], Asunción Bautista [a], Beatriz Galiana [b]

[a] Department of Materials Science and Engineering, IAAB, Universidad Carlos III de Madrid. Avda. Universidad 30. 28911 Leganés, Madrid, (Spain).

[b] Physics Department, Universidad Carlos III de Madrid. Avda. Universidad 40. 28911 Leganés, Madrid, (Spain).

*Corresponding author: mfalvare@ing.uc3m.es; Tel.: +34916249482

Abstract

Epoxy powder coatings were functionalized with nanosilica to improve wear resistance. Ten different organic coatings were studied: 0.25-1% (by wt.) of SiO_2 nanoparticles (both hydrophilic -HL- and hydrophilic -HB-) were added to epoxy powders. The homogeneity of the distribution of the silica nanoparticles in the epoxy powder matrix was achieved with an innovative ball-milling mixing method. This homogeneity was confirmed through transmission electron microscopy (TEM) observations. Powder coatings were sprayed and cured on steel sheets. The wear resistance of the coatings was evaluated in reciprocating wear equipment, measuring the depth and the width of the wear tracks obtained by an optoelectronic microscopy. Results reveal very significant improvement in wear resistance, with the best wear performance being observed for the epoxy reinforced with 0.75%HB SiO_2 nanoparticles. This is related to the enhanced crosslinking of the matrix in the coatings due to SiO_2, as shown by the mechanical properties. The curing kinetics of the functionalized epoxy powders was studied by non-isothermal differential scanning calorimetry (DSC). Activation energies (E_a) calculated from DSC are related to in the diffusion-controlled reactions.

Keywords

Epoxy powder coating; Silica nanoparticles; TEM; Curing kinetics; Wear resistance.

1. Introduction

Organic coatings have an important role in the protection of metals against corrosion. It is important to assure their mechanical and wear resistances in order to maintain their physical barrier effect and to extend their service behavior. Regarding the different types of polymers used as organic coatings, epoxy resins stand out because of their mechanical properties, as higher stiffness and wear resistance and lower friction [1-4]. However, the resistance of pure epoxy is often not enough to guarantee its durability during its service life. Up to now, the mechanical properties can be improved thanks to the addition of nanofillers that provide increased hardness, stiffness and wear resistance to the epoxy liquid coatings [2,4], with silica being one of the most used nanofillers to improve these coatings [1,5-7] thanks to its good chemical stability and ease of dispersion.

Powder organic coatings have clear advantages in comparison with liquid coatings as they do not contain volatile organic solvents and only a small amount of material is lost during the electrostatic spray process [8,9]. However, there is little literature regarding the functionalization of powder organic coatings to improve their properties compared to that already published in this line for conventional liquid coatings. For instance, focusing on SiO_2 additions to liquid epoxy coatings, it has been shown that nanoparticles improve their abrasion resistance more effectively when compared to microparticles [10]. On the other hand, SiO_2 nanocontainers improve the wear resistance of liquid coatings through the hardening of the material [11].

The few studies already carried out about functionalized powder coatings have proved that the addition of nanoparticles improves the adhesion to substrate and the hardness of polyester powder coatings [12-13]. Moreover, the hardness [14] and impact resistance [15] of epoxy powder coatings can be enhanced as well through nanoadditions. With SiAlON [16] and silicoaluminates [17] nanoparticles, epoxy powder coatings under abrasion tests have been shown to be able to increase their hardness and stiffness [16] and to modify their viscoelastic properties [17]. Under erosive wear conditions, SiC [18], Al_2O_3 [18], or silicates [19], have shown that functionalizing powder epoxy resins with micrometric particles is also positive, with the fraction and size of fillers being extremely important [18]. Initial findings about the effect of SiO_2 nanoparticles on wear properties of powder organic coatings have already been tested in polyester resins [20].

At any rate, all of the research studies related to the addition of nanoparticles to organic coatings clearly underline the importance of embedding the particles properly

into the polymeric matrix. A homogeneous distribution, a correct nanoparticle-matrix interaction [5] and avoiding the formation of agglomerates of nanoparticles [21] are of great importance in order to optimizing the properties of organic coatings. However, the mixing methods used for adding nanoparticles liquid organic coatings [22]. cannot always be used with powder organic coatings. To date, most of the mixtures of powder organic coatings are made by extrusion [14,15,17,23-25]. The ball milling mixing method is an alternative to mixing the materials for the powder coating without temperature [20] and without having to grind the powder again after the mixing, which make it more economical than the extrusion. It can be considered a quite innovative method as there are very scarce precedents in the literature about the use of this method to manufacture functionalized organic powders for coatings [16,20]. Moreover, to the best of our knowledge, it is the first study that uses this method for introducing silica nanoparticles in epoxy powders.

An aspect that is usually overlooked regarding SiO_2 nanoparticles is their nature. As initially manufactured, they are hydrophilic due to the freely accessible silanol groups (Si-OH) on their particle surface. A post-treatment step is required to transform them into hydrophobic [26]. A very limited number of research studies compare both of them [27]; for instance, excellent dispersion and enhanced mechanical performance are found for hydrophobic SiO_2 with a certain polyurethane matrix, while hydrophilic ones lead to a lubricating behavior [27]. Although epoxy resins are often considered as hydrophilic [28], commercial powder organic coatings generally have fillers and pigments, so the hydrophilic nature of the whole coating is not always clear.

The aim of this investigation is to manufacture epoxy-based powder coatings with SiO_2 nanoparticles through ball milling with improved wear performance, ensuring a good homogeneity in their distribution in the epoxy powder coating. In addition, the difference between hydrophilic and hydrophobic nanoparticles will be studied. Finally, an approach to the curing kinetics of those coatings will be presented.

2. Experimental

2.1 Materials and samples preparation

A commercial epoxy powder provided by Cubson International Consulting S.L. (Humanes de Madrid, Spain), was used for the manufacturing of the organic coatings. Silica nanoparticles were purchased from Aerosil® (Evonik, Essen, Germany). Both hydrophilic (Aerosil® 90, with Si-OH groups on the surface) and hydrophobic (Aerosil®

R202, with Si-CH_3 groups on the surface) nanoparticles were used. Their properties are shown in Table 1.

Table 1: Properties of silica nanoparticles (according to the supplier).

	Model	Nomenclature	Surface area ($m^2 \cdot g^{-1}$)	Average size (nm)
Hydrophilic SiO_2	Aerosil 90	HL	75-105	20
Hydrophobic SiO_2	Aerosil R202	HB	80-120	14

For mixing the matrix and the reinforcements, a two-body planetary ball mill Pulverisette 5 was used (Fritsch, Idar-Oberstein, Germany) for 10 min. During the ball milling process, the collision with hard balls promotes the mixing of the nanoadditions with the painting powders. In this case, stainless steel balls with 8 mm diameter were used and the ratio of material/balls was 1:10. All the mixtures were made under dry conditions in a vessel with a volume of 250 ml.

Ten different organic coatings were studied: the as received epoxy powder coating (AR), the AR milled without nanoparticles (0%), 4 different mixtures with different percentages of hydrophilic SiO_2 nanoparticles (0.25%HL, 0.5%HL, 0.75%HL, 1%HL) and 4 different mixtures with the same percentages of hydrophobic SiO_2 nanoparticles (0.25%HB, 0.5%HB, 0.75%HB, 1%HB). All percentages are expressed by weight.

Degreased carbon steel substrates (152 x 76 x 0.8 mm) were used (EspanColor S.L., Barcelona, Spain) to apply the different epoxy organic powders. The coating application was performed with an electrostatic spray gun (Pulverizadora Manual Easyselect) with a control unit OPTITRONIC (ITW GEMA, San Galo, Switzerland). The voltage source was 100 kV DC. The curing was carried out in an oven according to the manufacturer's conditions (180 °C, 15 min). The thickness was about 70±10 µm for the all epoxy powder coatings, measured with a thickness gauge (Elcometer 456, Manchester, UK).

2.2 Characterization and testing

A study of the homogeneity of the distribution of the silica nanoparticles in the epoxy powder was carried out by Transmission Electron Microscopy (TEM). Also, the interaction between nanoparticles and epoxy matrix was analyzed. The samples were characterized by means of high resolution TEM (HRTEM), Z-contrast Scanning TEM (STEM) mode using a high angle annular dark field (HAADF) detector and high resolution energy dispersive X-ray emission (EDS). TEM measurements were performed at 200 keV on Philips Tecnai F20 (Philips, Eindhoven, The Netherlands). The samples were prepared using the carbon grid, selecting those powders with highest amount of silica.

In order to evaluate the wear resistance of the manufactured organic coatings, sliding wear determination was performed using a UMT Tribolab tribometer (Bruker, Billerica, USA). A stainless steel ball (Ø = 6 mm) was used as countermaterial. The tests were carried out for 10 min, under dry conditions, using a load of 5 N and a frequency of 10 Hz. Three tests were made on each sample. All the tests were performed at room temperature (25 ^{o}C approximately). The coefficient of friction (COF) was also measured during each wear test.

Wear tracks were analyzed with Olympus DSX500 optoelectronic microscopy (Olympus Corporation, Tokyo, Japan). The depth and the width of each wear track were measured. At least six measurements were made in each wear track. Micrographs of the worn coatings were also taken using this technique. Scanning electron microscopy (SEM) was also used to study the wear mechanisms of the organic coatings. Images were taken with a 10 kV electron beam and two different detectors: an Everhart-Thornley Detector (ETD) and a Circular Backscatter Detector (CBS).

The contact angle and the surface energy of the cured epoxy coatings were measured with a Dataphysics OCA15 plus goniometer and a SCA20 software (DataPhysics Instruments GmbH, Filderstandt, Germany). Three liquids with different polarities were used for determining the surface energy: water, diiodomethane and glycerol. The Owens-Wendt-Rable-Kaelble (OWRK) method [29,30] was used to calculate the dispersive and the polar components. Nine measurements were carried out for each of the liquids used for testing on each coating.

The stiffness, the universal hardness (HU) and the plastic work (W_{plast}) of all the organic coatings were measured to evaluate their mechanical properties with a universal hardness tester ZHU 2.5 (Zwick Roell, Ulm, Germany). The conditions established

were: a load of 5 N, a load application speed of 1 mm·min^{-1} and a load removal speed of 10 mm·min^{-1}. Nine measurements were made on each epoxy-based cured coating.

The glass transition temperature (T_g) of the cured organic coatings was determined by a differential scanning calorimeter (DSC), model 822 (Mettler Toledo GmbH, Greifensee, Switzerland). Nitrogen was used as purge gas with a 35 ml·min^{-1} flow and all the samples were tested in a temperature range of 25-125 °C. Aluminum crucibles of 40 µl were used with a sample weight of 10.5±0.5 mg. A heating rate of 20 °·min^{-1} was used.

A kinetic study on the curing of the epoxy powders was carried out in order to study if there is an effect of the SiO_2 nanoparticles in the curing process of the epoxy powder coating. A DSC was also used to calculate the different thermal measurements. Aluminum crucibles of 40 µl were used with a sample weight of 10.5±0.3 mg. Nitrogen was used as purge gas with a 35 ml·min^{-1} flow and all the samples were tested in a temperature range of 25-250 °C. Three different tests were carried out for each organic coating, at 3 different heating rates: 5, 10 and 20 °·min^{-1}.

Two different methods were used to determine the activation energy (E_a) of the cure reaction of each organic powder coating: the Kissinger method and the Model Free Kinetics (MFK) method. The Kissinger method is defined by Eq.1 [31] where E_a is the activation energy (J·mol^{-1}), T_p is the peak of curing curve (K), β is the heating rate (°·min^{-1}), R is the gas constant (J·mol^{-1}·K^{-1}) and C is a constant. This method calculates a constant E_a throughout the whole polymer coating curing process. The MFK method [32,33], however, supposes an E_a that varies with the curing degree (α) and was calculated with the STARe software (Mettler Toledo GmbH, Greifensee, Switzerland).

$$ln\left(\frac{\beta}{T_p^2}\right) = \frac{-E_a}{RT_p} + C \quad (1)$$

3. Results and discussion

3.1 Interaction of silica nanoparticles with the epoxy powder

Low magnification TEM images together with STEM measurements were acquired to characterize the SiO_2 nanoparticles distribution in the epoxy powder. TEM images were used to determine the size of the SiO_2 nanoparticles, as well as their distribution in the epoxy. Although the manufacturer provides an average particle size (shown in Table 1), the nanoparticle size distribution is very wide. Fig. 1 gathers representative TEM images of the HL and HB SiO_2 nanoparticles. As can be observed in Fig. 1a and Fig.

1b, in general, HB nanoparticles have a more uniform size and are smaller than HL nanoparticles. For the case of HL nanoparticles, there is a wider particle distribution with nanoparticles that measure up to about 150 nm diameter (Fig. 1a). In Fig. 1c and Fig. 1d, two average sized HL and HB isolated nanoparticles are shown. The diameter of these two specific silica nanoparticles are 52 nm and 40 nm, respectively. Regarding the morphology of the SiO_2 nanoparticles, both HL and HB are very similar, as both are amorphous silica (since no crystalline planes have been detected) and have a very rounded shape.

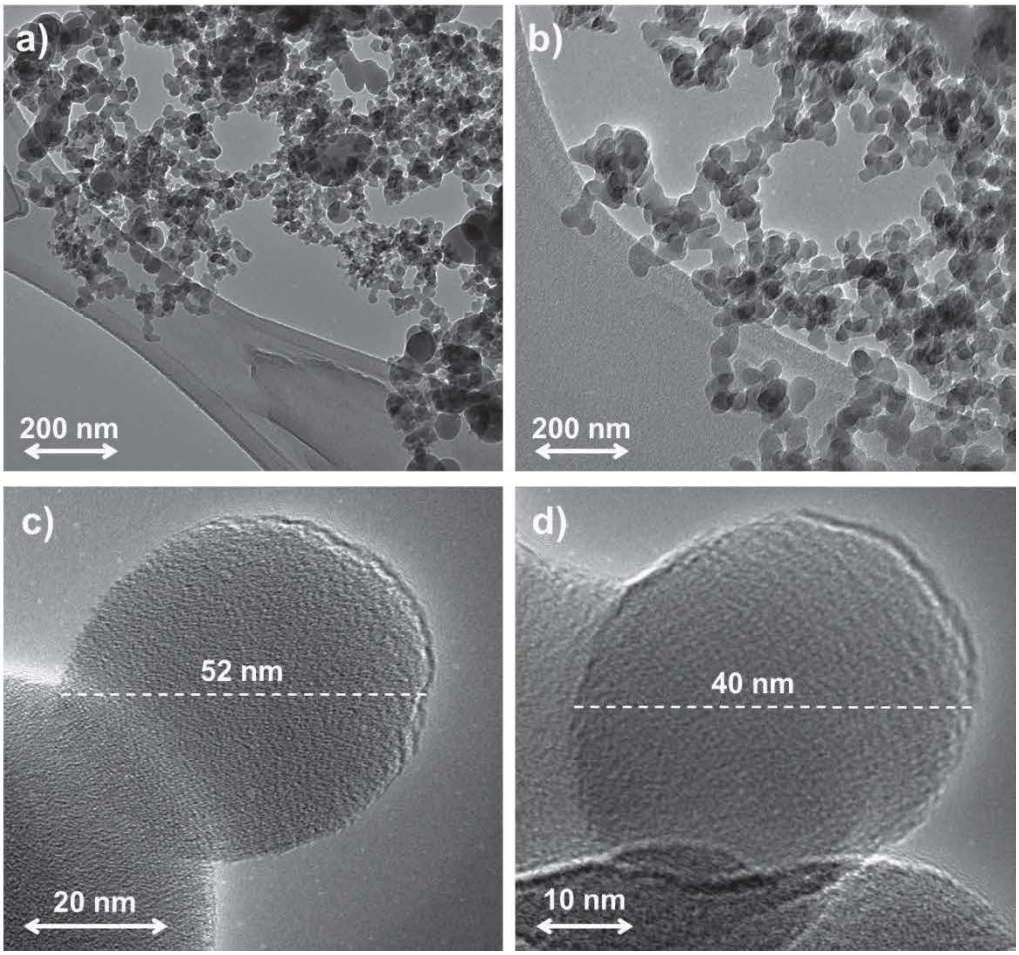

Fig. 1: Bright-field TEM images of the SiO_2 nanoparticles: a) HL and b) HB SiO_2 nanoparticles distribution; c) HL and d) HB isolated nanoparticles.

In order to study this in detail, the dispersion of silica nanoparticles in the epoxy matrix, chemical compositional maps and EDS spectra of the nanoparticles have been achieved using EDS together with Z-contrast images. Fig. 2 shows the STEM analysis of the 1%HL (Fig. 2a) and the 1%HB (Fig. 2b) organic coatings. The darker areas

correspond to the organic material (epoxy powder) and the lighter areas to inorganic materials (either nanoparticles or fillers).

Fig. 2a shows a STEM image of 1%HL powder, together with an EDS compositional maps of Si (K) and O (K) of the region limited by the red square on the epoxy powder coating (Fig. 2b). Analyzing the data presented, it is possible to easily determine the existence of several SiO_2 nanoparticles sized below 100 nm and embedded in the epoxy. Those nanoparticles are distributed homogeneously in the epoxy matrix. In Fig. 2c a STEM image can be seen of the 1%HB organic powder and an EDS spectrum of the region delimited by the white circle (20 nm radius), revealing that it is SiO_2 (Fig. 2d). In this case, the contrast of the HB SiO_2 nanoparticles with respect to the matrix is lower. This is due to the smaller size of HB nanoparticles, as demonstrated in Fig. 1. These results confirm a good homogeneity in the distribution of nanoparticles since no agglomerates are observed.

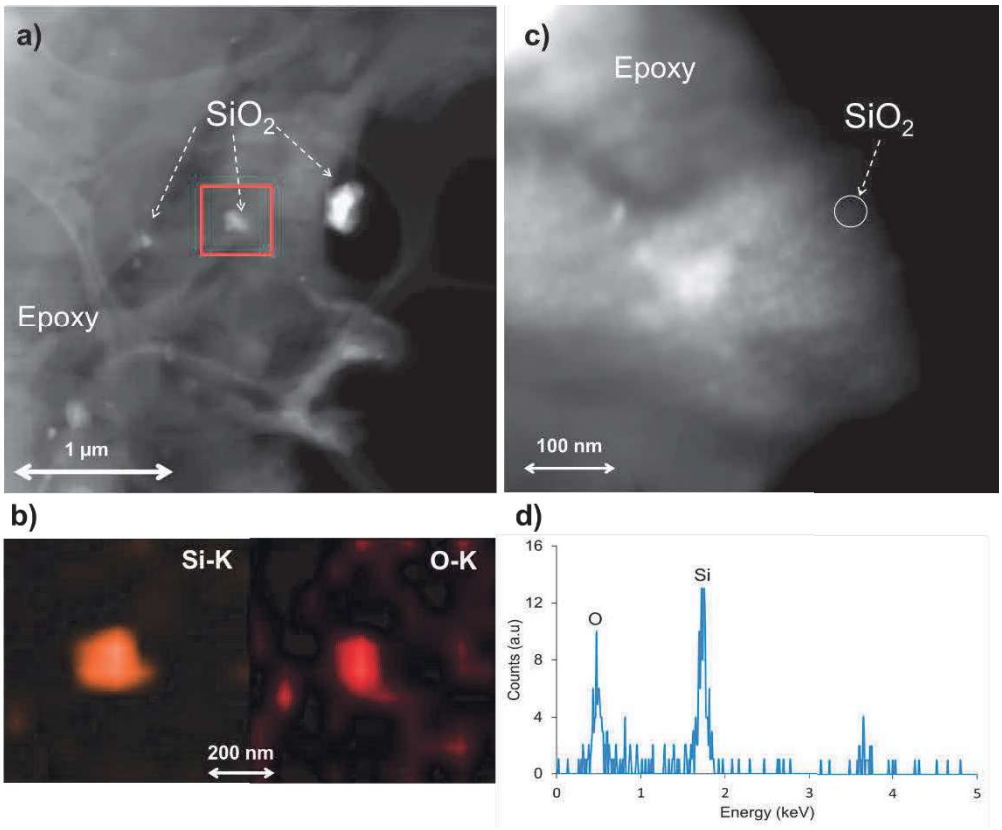

Fig. 2: a) STEM images of 1%HL organic coating; b) EDS compositional maps of Si (K) and O (K) of the region limited by the red square on the epoxy powder coating in figure a; c) 1%HB organic coating; d) EDS spectrum of a SiO_2 nanoparticle in figure c.

Fig. 3 shows the epoxy powders with a HL (a) and a HB (b) nanoparticle respectively, after the ball milling process. These samples correspond to the epoxy powder that contains the highest percentage by weight (1%) of SiO_2 nanoparticles. An EDS spectrum was carried out on the nanoparticles to verify that they are SiO_2. Fig. 3c gathers the EDS spectrum measured at the red cross plotted in Figure 3a. As can be observed, O-K line (0.48 keV) and Si-K line (1.71 keV) are clearly measured. The same spectrum has been achieved for HB isolated nanoparticles (not shown here). The quantification of the spectrum reveals a composition compatible with SiO_2. It can be seen again how HB nanoparticles are generally smaller compared to HL nanoparticles.

Moreover, Fig. 3 allows confirming how both nanoparticles are embedded in the epoxy powder, so the interaction of the nanoparticles with the epoxy matrix has been achieved correctly. Hence, the innovative mixing method (ball milling) selected has provided a correct distribution of the nanoparticles in the polymer, without agglomerates (Fig. 2) together with good interaction between nanoparticles and epoxy (Fig. 3), which can lead to a correct curing process of the organic coating and to achieving better properties in the coating.

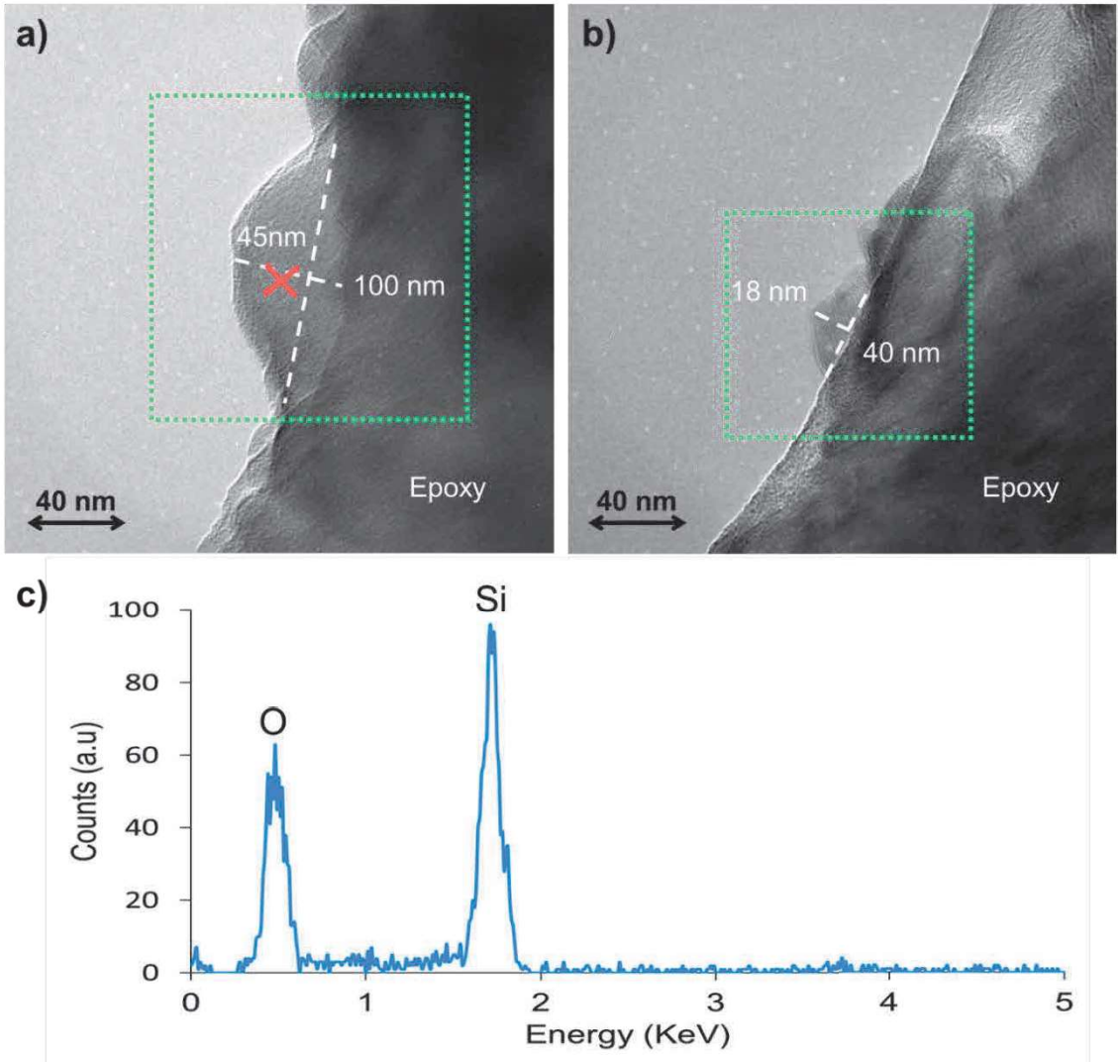

Fig. 3: a) HL and b) HB SiO_2 nanoparticles embedded in the epoxy powder after ball milling. c) EDS spectrum of a SiO_2 nanoparticle.

3.2 Influence of silica nanoparticles on the properties of the organic coating

The main purpose of the addition of SiO_2 nanoparticles in these functionalized epoxy coatings is to increase their wear resistance. In order to characterize the wear resistance and to study the influence of the nanosilica on the wear mechanism, all the wear tracks of the different epoxy coatings were analyzed after testing. The morphology of the tracks was analyzed with optoelectronic microscopy obtaining images like those shown in Fig. 4.

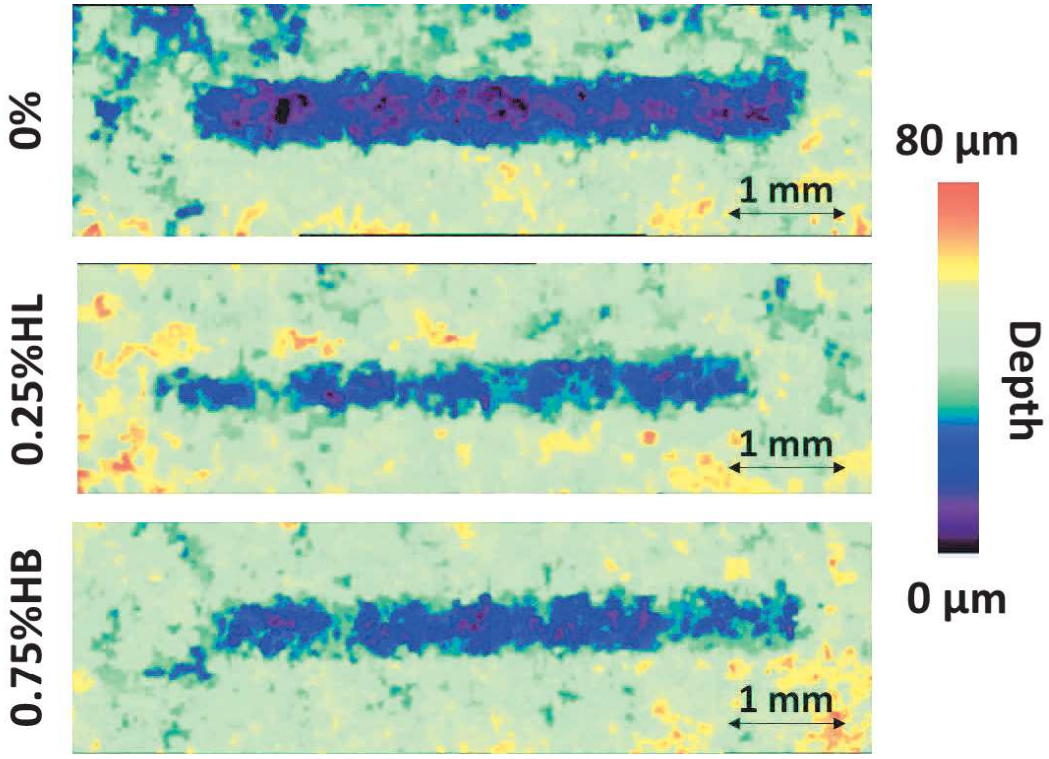

Fig. 4: Wear tracks of 0%, 0.75%HB and 0.25%HL organic coatings.

The most relevant results obtained from the analysis of images of the track such as those in Fig. 4 are plotted in Fig. 5. The data presented correspond to the average values for the depth and the width of all the wear tracks and the standard deviation of the measured parameters. It can be seen that the greatest differences are observed in the depth rather than in the width of the wear tracks, although the evolution of both parameters is related. The width of the track is clearly limited by the diameter of the ball (countermaterial), so it is less sensitive to the aggressiveness of the wear attack.

When comparing the wear tracks in the AR and the 0% coatings, it can be checked that they have similar depth and width values. This indicates that the ball milling process has not affected the wear properties of the epoxy material. As silica nanoparticles are added, both values decrease (Fig. 4), indicating improved wear resistance.

However, different behaviors can be observed for both types of SiO_2 nanoadditions. In the case of coatings with 0.25% HL nanoparticles, the depth of the track is already 10 µm lower than the depth in non-functionalized coatings. This value remains practically constant for 0.5%HL coatings, and subsequently, for higher amount of HL additions, the depth increases slightly. The same trend can be observed for the width values of the wear tracks, although in a less marked way. Regarding the organic coatings that

contain HB nanoparticles, the depth of the wear track is progressively reduced when the amount of silica increases. The best result is obtained for the 0.75%HB, although the improvement achieved from the 0.25% addition is noticeable. However, the 1%HB coating experiences considerable worsening in its wear performance, although the TEM results (Figs.2b and 3b) can allow us to discard the presence of the "agglomerates/aggregates" that often cause a decrease in the performance of the coating when the nanoparticles are added in high amounts [6,21].

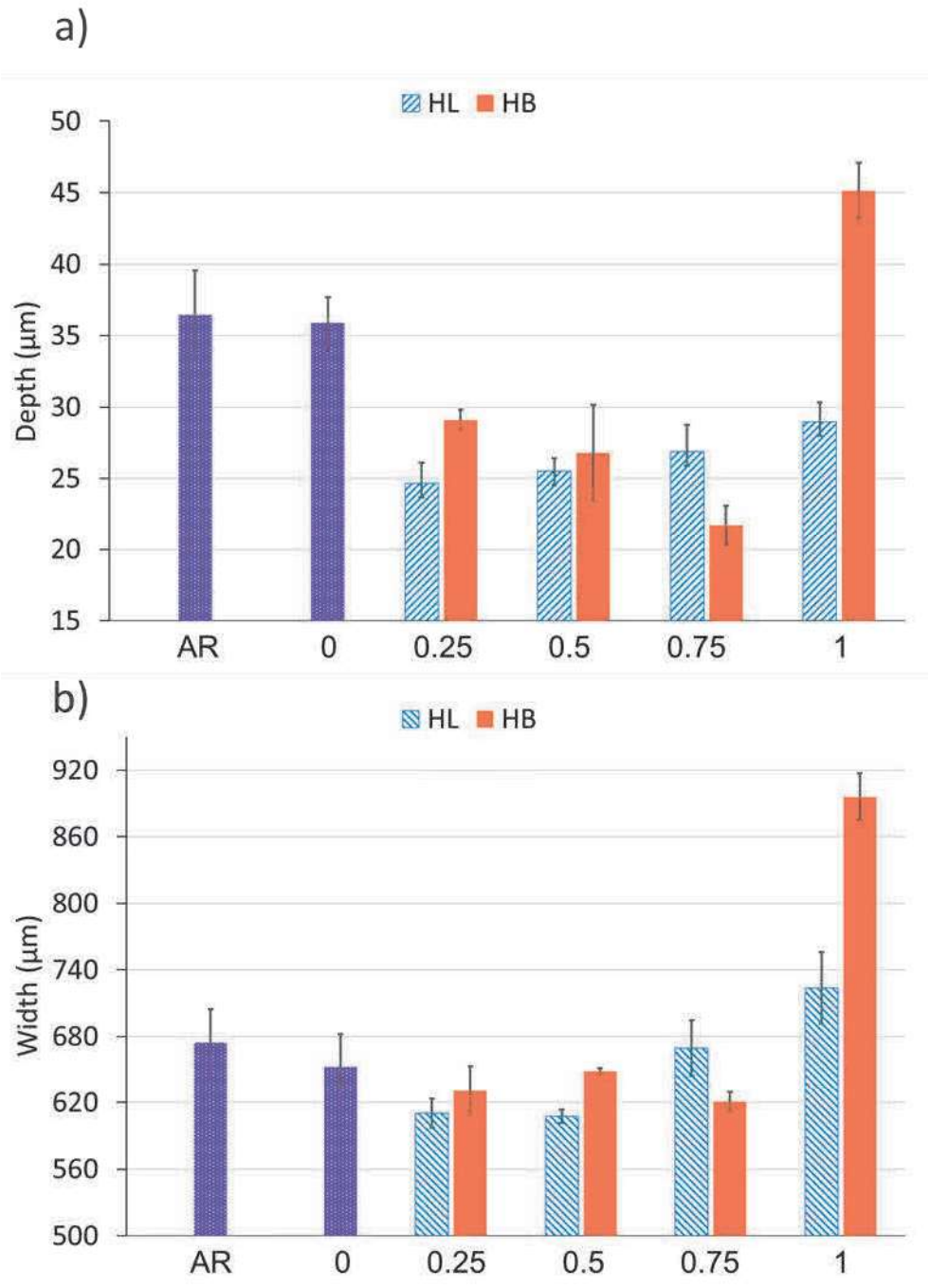

Fig. 5: Wear track analysis: a) depth and b) width of the wear track of the functionalized and non-functionalized studied epoxy coatings.

The wear mechanisms can explain the differences found between the performance of the different coatings studied. In Fig. 6, SEM images of the wear tracks of the 0% (a and b), 0.75%HB (c and d), 1%HL (e and f) and the 1%HB (g and h) are observed. The 0% coating clearly shows cracks transverse to the sliding direction, especially appreciated at the highest magnification (Fig. 6b). This failure mode is similar to those reported in other studies [34]. No scratches, typical of an abrasive wear mechanism, are found (Fig. 6a). In polymer-on-metal sliding, there is a natural tendency for polymeric material to be transferred to the metallic countermaterial. The flat worn surface of 0% (Fig. 6a) can correspond to a soft material, where transfer (wear) of material takes place more easily. Material transferred during each stroke of the cycle is loosened and could be removed by the reverse stroke, with the removal of material being more dominant under high contact stresses. Material loss reveals that the adhesive wear mechanism plays a main role in the damaging process. Shear deformations at adhesive seizure are commonly associated with the fracture of a polymer surface as that shown in Fig. 6a [17].

All coatings but 1%HB show the same performance just discussed for the 0%. As an example, the 0.75%HB (Fig. 6c and 6d) and the 1%HL (Fig. 6e and 6f) organic coatings show the same tensile cracks on their surface than the 0% (Fig. 6b) and with the rest of the epoxy coatings (not included in Fig. 6). Differences in wear depth results (Fig. 5a) could be related, for instance, to the mechanical properties of each individual coating. The addition of 1%HL SiO_2 nanoparticles (Fig. 6e), which are adequately incorporated to the epoxy matrix (Fig. 3), makes the transfer of material more complicated, and the worn surface changes macroscopically. Evidently, the bonding between SiO_2 nanoparticles and the epoxy increases the integrity of the composites, leading to some deformation on the surface and less removal of material.

On the other hand, 1%HB (Fig. 6g and 6h) shows a completely different behavior. The transverse cracks are bigger and deeper than in the other materials, and longitudinal cracks (clearly observable at low magnification) also appear. This behavior suggests a higher brittleness for this coating, which could have negatively affected its wear performance (Fig. 4). Other authors [35,36] have found similar situations in epoxy polymers with an amount of SiO_2 nanoparticles between 3-6 % by wt.

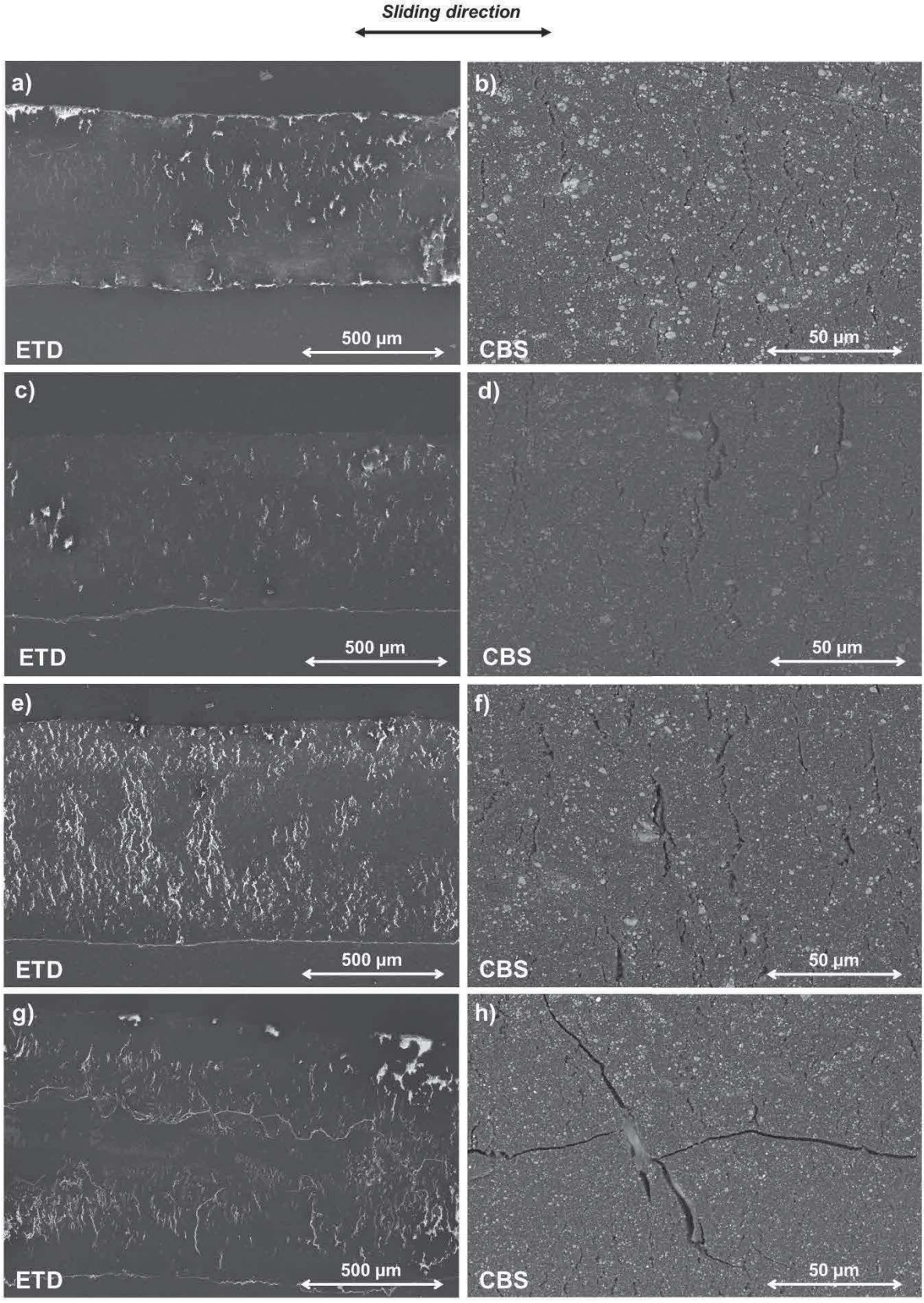
Sliding direction
a)
ETD
500 µm
b)
CBS
50 µm
c)
ETD
500 µm
d)
CBS
50 µm
e)
ETD
500 µm
f)
CBS
50 µm
g)
ETD
500 µm
h)
CBS
50 µm

Fig. 6: Wear tracks of 0% (a and b), 0.75%HB (c and d), 1%HL (e and f) and 1%HB (g and h) organic coatings.

In Fig. 7, the evolution of COF obtained during some of the wear tests (600 s) are shown. In all cases, 3 different stages in the COF can be observed: a first stage where the COF stays low and grows slightly (typical of sliding conditions), a second stage where COF grows very fast (the beginning of the wear) and finally, a third stage, where the COF is again more or less constant during the rest of the wear test. Other authors [37] have also found that COF during wear test grows from the start and then remains constant. All the organic coatings studied have a similar behavior since they present the 3 stages, but these stages start and end at different times, thus defining the wear resistance of each epoxy coating. The original epoxy coating (AR) and those containing HL nanoparticles present a short first stage before the wear starts (at approximately 50 s). Nevertheless, the organic coatings with HB nanoparticles delay the appearance of the wear up to 4 times more than for the other coatings (at 230-280 s approximately). This can be observed because the sliding stage (first stage) is much longer due to the mechanical properties of the coating, as it will be discuss later. Regarding the 0.75%HB, which is the organic coating that presents less deep tracks (Fig. 5a), and this corresponds to a delay in the onset of wear. The 1%HB can be seen to further delay the beginning of the wear, but as seen in Fig. 6h, the wear mechanism could result in being more aggressive due to the observed trend of developing brittle cracks. Those higher wear losses in the 1%HB (Figure 4) can also be related to the marked fluctuations observed in the third stage of COF (Fig. 7).

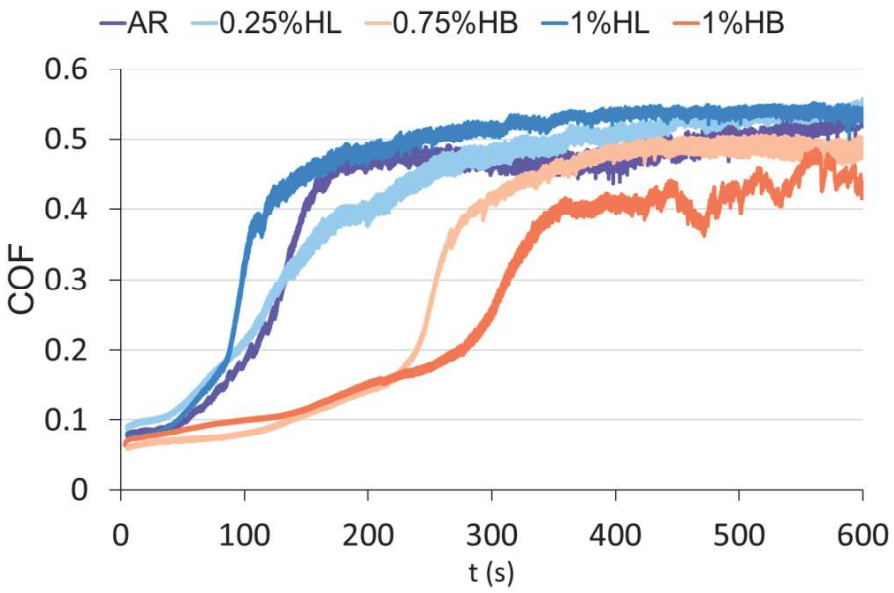

Fig. 7: COF evolution of selected organic coatings during wear test.

Regarding the final COF values, there are no major variations between the different epoxy coatings. The final COF of the organic coatings (approximately 0.5) corresponds to similar values studied in other epoxy systems [1,36]. The lowest value obtained was for 1%HB and the maximum for the 1%HL. Differences in the COF value between AR and 0.75%HB do not exist, but the delay in the beginning of the wear of the coating makes 0.75%HB the best option out of all the coatings studied.

The results on the wear performance found in the coatings studied can be understood bearing in mind those corresponding to their mechanical properties (Fig. 8). It has been shown that the curing degree of SiO_2 containing epoxy resins affect the final mechanical properties [18]. As expected, SiO_2 nanoparticles have converted the epoxy into a more rigid and brittle matrix [7,28,38], and with greater hardness as well [39]. The hardness and the stiffness increase with the percentage of SiO_2 and consequently, W_{plast} decreases when the percentage of silica increases (Fig. 8). It can be assumed that bonds are formed between nanoparticles and the polymer, immobilizing polymeric chains and increasing the crosslinking of the polymer [40] and the stiffness of the matrix around the particles. The W_{plast} is related to the stiffness: the higher the stiffness of the organic coating, the lower its W_{plast}. The increase of stiffness confirms that the crosslinking of the polymer has been clearly fostered by the silica additions, increasing this effect as the amount of nanoreinforcements in the coating is also increased. These results confirm the TEM observations that a good interaction between nanoparticles and epoxy has been achieved, with a homogeneous distribution of nanoparticles and

finding neither aggregates nor agglomerates. This distribution promotes a high amount of interface capable of transferring stresses from the matrix to the fillers [41]. The relatively similar surface of the HB particles added in comparison to that of HL particles (Table 1 and Fig. 1) could be related to similar results observed in Fig. 8 for the mechanical properties of the coating when identical amounts of hydrophilic and hydrophobic particles are added. It is true that the effect of the particles on the crosslinking not only depends on the amount of the interface, but also on the quality of the interaction between them and the matrix. From the results in Fig. 8, no clear advantage of one kind of particle or another can be observed.

The positive influence on wear resistance of the organic coating is also related to the nanoadditions, as has previously been reported for other systems [16,40,42]. The improvement on the wear results observed in Figs. 4 and 5 could be related to this increase on the crosslinking of the polymers caused by the nanoparticles that the mechanical tests have demonstrated (Fig.8). The increase of the crosslinking of the matrix allows a better stress transfer. The longer sliding stage of COF (Fig. 7) observed for 0.75%HB and 1%HB also relies on the cross-linking phenomenon and its enhancement due to the presence of nanosilica.

However, a high level of crosslinking can lead to an embrittlement, as occurs with the 1%HB coating (Fig. 6h). For this coating, hardness and stiffness increase somewhat more than the other coatings (Fig. 8a) and it exhibits a clear decrease in its W_{plast}. The largest amount of hydrophobic particles studied promotes such an intense curing process that the wear mechanism changes, and the wear resistance decreases. This type of reduction in the in-service performance due to the addition of a large amount of particles has been previously reported [4].

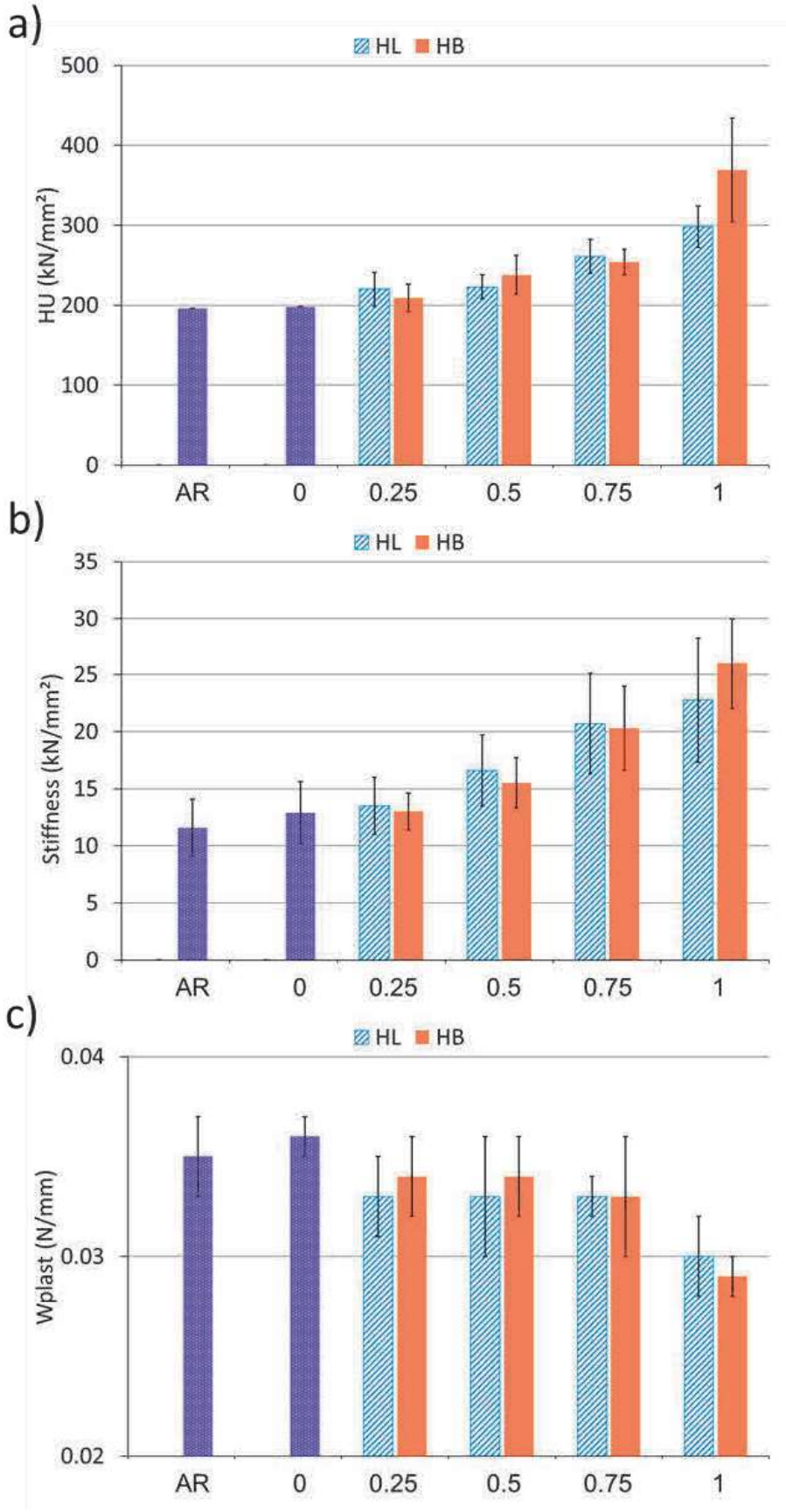

Fig. 8: a) HU, b) stiffness and c) W_{plast} values of all epoxy coatings.

To obtain more information about how the hydrophilic or hydrophobic nature of nanoparticles can affect their interaction with the epoxy coating, contact angles were measured and the surface energies were calculated on the cured coatings. Table 2 collects the static contact angles with water and the surface energies of the AR, 0.75%HL, 0.75%HB, 1%HL and 1%HB cured organic coatings. As the dispersive part of the surface energy is larger than the polar part, it can be concluded that epoxy organic coating surface has a predominantly hydrophobic nature. It is well-known that epoxy resins have several polar groups that provide them with hydrophilic properties. However, the presence of meaningful amounts of the other different chemical compounds in the powders as well as the influence of the surface roughness in the hydrophobicity can explain the obtained results. The values in Table 2 are similar to other studies of epoxy organic coatings [1,5]. The difference between the contact angle results obtained for the three studied organic coatings is practically insignificant. As the amount of nanoparticles used is much reduced, these hardly noticeable effects are logical. Moreover, as no huge deviation in data was obtained, the homogeneity of the coating can be considered to be in line with the good dispersion observed for the nanoparticles (Fig. 2).

Table 2: Contact angle (with water) and surface energy of AR, 1%HL and 1%HB.

	Contact angle (°)	**Surface energy ($mJ \cdot m^{-2}$)**		
		Total	**Dispersive**	**Polar**
AR	79±2	39±3	35±3	4±1
0.75%HL	78±1	39±2	34±2	5±1
0.75%HB	80±2	39±3	35±3	4±2
1%HL	78±2	39±3	34±3	5±1
1%HB	81±4	38±3	34±2	4±1

The non-clear hydrophilic or hydrophobic character of the resin is in accordance with the absence of dramatic differences between coating with HB and HL particles when they are added in small amounts (Fig. 5 and 8). Although the AR coating can be considered more hydrophobic than hydrophilic, the results in Table 2 suggest that the resin has components that can promote positive interactions with HB particles as well as with HL particles. The higher ability of 1%HB to promote hardening (Fig. 8) could be related to the lower size and higher surface of these particles in comparison to HL (Table 1 and Fig. 1). In previous studies, it has been concluded that the lower the

nanoparticle size, the higher the increase produced on the properties [10]. However, the size of the particles is not so different, and a certain influence of the hydrophobic nature of the particles in promoting a better anchoring of the matrix cannot be discarded.

3.3 Insight on curing kinetics

Table 3 shows the different glass transition temperatures (T_g) obtained by DSC for the different epoxy cured coatings. Very small differences can be appreciated among all the organic coatings, since T_g values lie at 95±1 ^oC. No effect on T_g is found due to the different SiO_2 nanoparticles (HL and HB). These results also address the idea of the homogeneity of the mixture and are consistent with the results obtained by TEM (Figs. 2 and 3). If the T_g had decreased with SiO_2 nanoparticles, it would have meant that agglomerates were present, not allowing a good crosslinking of the organic coating and consequently, the mechanical properties would have also gotten worse [38,43].

Table 3: T_g values of all epoxy-based coatings.

	T_g (^oC)
AR	95
0%	96
0.25%HL	94
0.5%HL	95
0.75%HL	94
1%HL	96
0.25%HB	95
0.5%HB	96
0.75%HB	95
1%HB	95

The curing kinetics of the coatings studied was evaluated in order to analyze if the crosslinking enhancements shown through wear (Figs. 4 and 6) and mechanical (Fig. 8) behavior can be appreciated. It is clear that nanoparticles and their dispersion can affect the curing of polymers [43]. There are very few studies related to the curing process of organic powder coatings, and they are mainly devoted to defining the temperatures of the process for polyester and polyester-epoxy coatings [13,44-46] or to the study of conversion of polyester coatings [47]. Using this technique, it has been

seen that calcium carbonate [13] and TiO_2 [25] nanofillers reduce E_a of polyester based resins.

As an example, some of the DSC curves obtained at 20 °·min^{-1} are shown in Fig. 9, although two other testing conditions (at 5 °·min^{-1} and 10 °·min^{-1}) were also used in order to allow the Kissinger and MFK methods to be applied. For all samples and all heating rates, two different peaks can be observed: the first peak (endothermic) corresponds to an enthalpy relaxation of the epoxy polymer (at 80 °C approximately) and the second peak (exothermic) corresponds to the curing reaction (epoxy crosslinking). This interpretation for the first peak can be verified because when a second scan is being done, this peak disappears. At any rate, enthalpy relaxation is a common phenomenon in polymers and is not relevant in this case. Moreover, silica nanoparticles do not seem to influence it, as has been already shown in previous studies [48]. As for the curing peak, it starts and ends at different temperatures, depending on the heating rate. In the case of the 20 °·min^{-1}, the cure peak begins at approximately 130 to 240 °C, as can be seen in Fig. 9, and at lower heating rates, the peak shifts to lower temperatures.

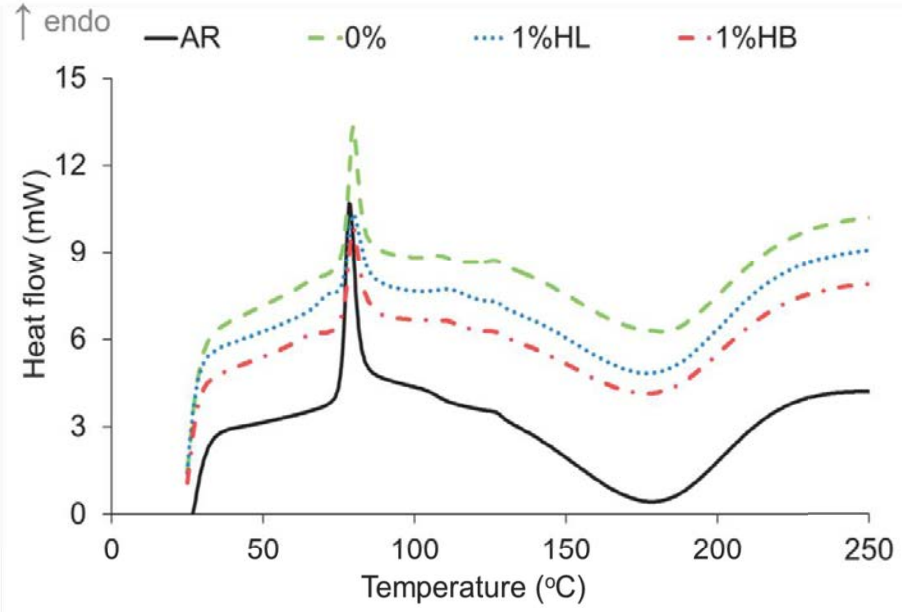

Fig. 9: Non-isothermal DSC curves (20°·min^{-1} heating rate) of AR, 0%, 1%HL and 1%HB epoxy powders.

Once the DSC curves were obtained, the curing peak was studied using the Kissinger and MFK methods. To calculate the E_a with the Kissinger method, Eq. 1 was used. The E_a value of the curing reaction was obtained by plotting $-\ln(\beta/T_p^2)$ vs. $1/T_p$. Table 4 collects the values of the peak temperature (T_p) obtained from the DSC curves necessary for the resolution of the Kissinger equation, and the E_a obtained for each epoxy powder coating. Kissinger assumes a first order reaction to calculate a constant E_a during the whole process, since this method assumes that the curing reaction is of order 1. The values obtained are similar to other epoxy systems also evaluated with the Kissinger method [49,50,51].

As many epoxy systems present a nth order reaction [52], the MFK method allows completing the information given by the Kissinger method described above. MFK is more complex, since more parameters are required and, besides that, the E_a changes according to the curing conversion, without the assumption of a particular order of the reaction model [53]. In Fig. 10, the E_a of all epoxy powder coatings are represented versus the curing conversion (%). The variation of E_a range out of 10 to 90% has been skipped over as it could be greatly affected by errors in the baseline [54]. The E_a values for AR and 0% organic coatings are plotted in both graphs in order to compare them more easily.

Generally, the first stages of conversion are related to chemically-controlled reactions while later stages are related to diffusion-controlled reactions. The well-known effect of nanoparticles, acting as interaction points with the resin chains [13], adsorbing them on the surface and creating high density layers [39], could provoke a catalytic effect, reducing E_a values. For the powder coatings studied, this effect is not detected and the changes in E_a found during the first stages of curing (Fig. 10) can be the results of complex influences. The curing of powder coatings proceeds under high viscosity conditions to avoid flow problems on the surface of samples. The viscosity of the resin during the curing is much higher than for liquid coatings, and additions of nanoparticles increase it. This effect could be responsible for the lower mobility of species during chemically-controlled first stages of reaction [55], shifting E_a to higher values when SiO_2 nanoparticles are present. Moreover, the effect of increasing reaction points, requiring more global energy per moll, cannot be ignored. The superposition of those effects can explain the observed values. At this stage of curing, there can be a mixed control of the curing reaction, where both the chemical process and the diffusion determine the rate of the polymerization process.

The diffusion control of the polymerization is later affected when species have to diffuse through the forming crosslinked network and the autocatalytic nature of epoxy curing reaction [53]. After a certain time, the value of E_a begins to stay almost constant. The values of the E_a at 50% curing degree (which is generally when the value of E_a is kept constant) of all epoxy based powders are shown in Table 4. This proposed mechanism is in accordance with the increased crosslinking that wear (Fig. 4) and mechanical properties (Fig. 8) show due to the effect of the addition of nanoparticles. Nanoparticles provoke an increase in the value during its evolution, as the example in Table 4 shows, clearly supporting the fact that a more crosslinked network exists when they are present, and, hence, diffusion of species (their mobility) is more complicated. 1% HB shows the highest values, implying that the degree of crosslinking is higher, affecting performance in a way that has even changed the wear mechanism (Fig. 6g and 6h).

Table 4: T_p (^{o}C) and E_a values calculated with the Kissinger equation (eq. 1) and MFK for all epoxy powder coatings.

	T_p (^{o}C)			E_a Kissinger (kJ·mol^{-1})	E_a MFK (kJ·mol^{-1})
β (^{o}·min^{-1})	**5**	**10**	**20**		
AR	150	165	180	65	67
0%	150	164	181	65	66
0.25%HL	151	165	181	65	72
0.5%HL	151	164	180	69	71
0.75%HL	150	164	179	69	74
1%HL	151	165	179	70	74
0.25%HB	150	164	180	68	70
0.5%HB	151	165	180	69	71
0.75%HB	151	164	180	70	71
1%HB	151	165	179	71	78

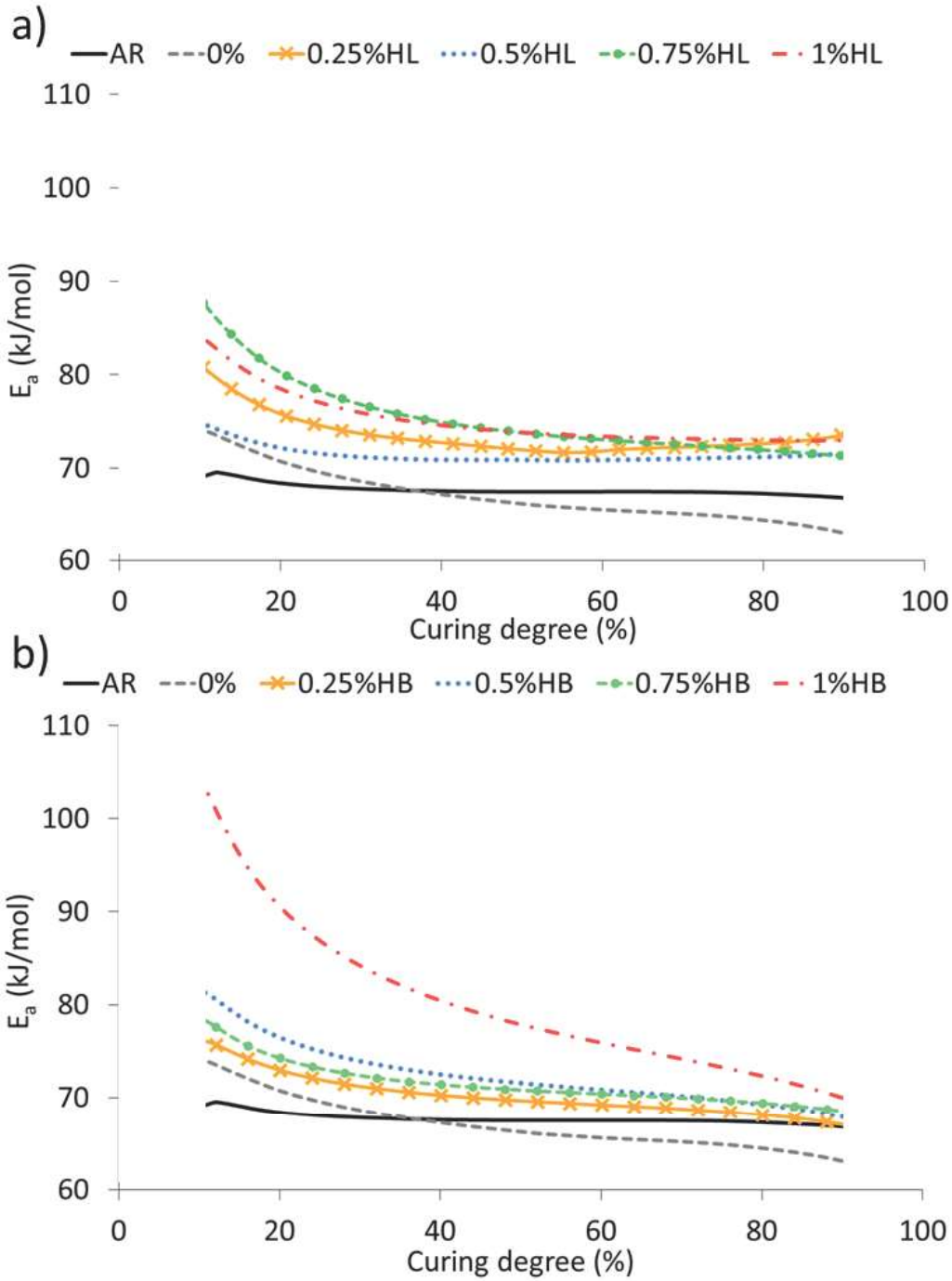

Fig. 10: E_a vs. curing degree by the MFK method for epoxy coating with: a) HL nanoparticles and b) HB nanoparticles.

4. Conclusions

In this work, two different silica nanoparticles were used to manufacture epoxy powder coatings for wear applications. After carrying out this investigation, the following main conclusions can be drawn:

- ✓ The ball milling method has allowed to obtain a good homogeneity for the dispersion of the silica nanoparticles in the epoxy powder coating. TEM studies have confirmed a correct embedding of the nanoparticles in the epoxy powder for both types of SiO_2.
- ✓ The small percentages of SiO_2 nanoparticles studied increase the wear performance of the epoxy based powder coating, due to the extension of sliding conditions during the wear test.
- ✓ The hardness and stiffness indicate that crosslinking is enhanced due to the addition of nanoparticles, increasing as the percentage of silica nanoparticles is higher. In the case of 1%HB, this increase is so high that coating becomes embrittled and the wear mechanism changes.
- ✓ The kinetic study carried out with DSC reflects the influence of the diffusion stages in the polymerization process.

Acknowledgements

The authors acknowledge Cubson International Consulting for their help with the coating process. This work was supported by Interreg SUDOE, through the KrEaTive Habitat project, grant number SOE1/P1/E0307 and the Spanish Ministry of Science, Innovation and Universities (MICINN) through the Spanish project RTI2018-101020-B-100.

References

1. M.H. Nazir, Z.A. Khan, A. Saeed, V. Bakolas, W. Braun, R. Bajwa, Experimental analysis and modelling for reciprocating wear behaviour of nanocomposite coatings, Wear. 416–417 (2018) 89–102. https:// doi.org/10.1016/j.wear.2018.09.011.

2. Y. Kang, X. Chen, S. Song, L. Yu, P. Zhang, Friction and wear behavior of nanosilica-filled epoxy resin composite coatings, Appl. Surf. Sci. 258 (2012) 6384–6390. https:// doi.org/10.1016/j.apsusc.2012.03.046.

3. S. Luo, Y. Zheng, J. Li, W. Ke, Slurry erosion resistance of fusion-bonded epoxy powder coating, Wear 249 (2001) 733–738. https://doi.org/10.1016/S0043-1648(01)00808-0.

4. J. Yu, W. Zhao, Y. Wu, D. Wang, R. Feng, Tribological properties of epoxy composite coatings reinforced with functionalized C-BN and H-BN nanofillers, Appl. Surf. Sci. 434 (2018) 1311–1320. https:// doi.org/10.1016/j.apsusc.2017.11.204.

5. M.A. El-Fattah, A.M. El Saeed, R.A. El-Ghazawy, Chemical interaction of different sized fumed silica with epoxy via ultrasonication for improved coating, Prog. Org. Coat. 129 (2019) 1–9. https://doi.org/10.1016/j.porgcoat.2018.12.023.

6. X.S. Xing, R.K.Y. Li, Wear behavior of epoxy matrix composites filled with uniform sized sub-micron spherical silica particles, Wear 256 (2004) 21–26. https://doi.org/10.1016/S0043-1648(03)00220-5.

7. M. Conradi, A. Kocijan, D. Kek-merl, M. Zorko, I. Verpoest, Mechanical and anticorrosion properties of nanosilica-filled epoxy-resin composite coatings, Appl. Surf. Sci. 292 (2014) 432–437. https://doi.org/10.1016/j.apsusc.2013.11.155

8. I. Stojanovi, V. Šimunović, V. Alar, F. Kapor, Experimental Evaluation of Polyester and Epoxy – Polyester Powder Coatings in Aggressive Media, Coatings 8 (2018) 98. https://doi.org/10.3390/coatings8030098.

9. A. Dupuis, T.H. Ho, A. Fahs, A. Lafabrier, G. Louarn, J. Bacharouche, A. Airoudj, E. Aragon, J.F. Chailan, Improving adhesion of powder coating on PEEK composite: Influence of atmospheric plasma parameters, Appl. Surf. Sci. 357 (2015) 1196–1204. doi:10.1016/j.apsusc.2015.09.148.

10. S. Palraj, M. Selvaraj, K. Maruthan, G. Rajagopal, Corrosion and wear resistance behavior of nano-silica epoxy composite coatings, Prog. Org. Coat. 81 (2015) 132–139. https://doi.org/10.1016/j.porgcoat.2015.01.005.

11. M. Rahsepar, F. Mohebbi, Enhancement of the wear resistance of epoxy coating in presence of MBT-loaded mesoporous silica nanocontainers, Tribol. Int. 118 (2018) 148–156. https://doi.org/10.1016/j.triboint.2017.09.023.

12. S.M. Mirabedini, A. Kiamanesh, The effect of micro and nano-sized particles on mechanical and adhesion properties of a clear polyester powder coating, Prog. Org. Coat. 76 (2013) 1625–1632. https:// doi.org/10.1016/j.porgcoat.2013.07.009.

13. M. Kalaee, S. Akhlaghi, A. Nouri, S. Mazinani, M. Mortezaei, M. Afshari, D. Mostafanezhad, A. Allahbakhsh, H.A. Dehaghi, A. Amirsadri, D.P. Gohari, Effect of nano-sized calcium carbonate on cure kinetics and properties of polyester/epoxy blend powder coatings, Prog. Org. Coat. 71 (2011) 173–180. https:// doi.org/10.1016/j.porgcoat.2011.02.006.

14. M. Sharifi, M. Ebrahimi, S. Jafarifard, Preparation and characterization of a high performance powder coating based on epoxy/clay nanocomposite, Prog. Org. Coat. 106 (2017) 69–76. https://doi.org/10.1016/j.porgcoat.2017.02.013.

15. H. Yu, L. Wang, Q. Shi, S. Jiang, G. Jiang, Preparation of epoxy resin/$CaCO_3$ nanocomposites and performance of resultant powder coatings, J. Appl. Polym. Sci. 101 (2006) 2656–2660. https://doi.org/10.1002/app.23908.

16. M.H. Moradi, M. Aliofkhazraei, M. Toorani, A. Golgoon, A.S. Rouhaghdam, SiAlON–epoxy nanocomposite coatings: Corrosion and wear behavior, J. Appl. Polym. Sci. 133 (2016) 1–13. https://doi.org/10.1002/app.43855.

17. A. Y. Grigoriev, G. V. Vaganov, V.E. Yudin, N.K. Myshkin, I.N. Kovaleva, I. V. Gofman, L.N. Mashlyakovskii, I. V. Tsarenko, Friction and wear of powder coatings of epoxy composites with alumosilicate nanoparticles, J. Frict. Wear 33 (2012) 101–107. https://doi.org/10.3103/S1068366612020043.

18. S. Luo, Y. Zheng, J. Li, W. Ke, Effect of curing degree and fillers on slurry erosion behavior of fusion-bonded epoxy powder coatings, Wear 254 (2003) 292–297. https://doi.org/10.1016/S0043-1648(03)00009-7.

19. D. Wang, E. Sikora, B. Shaw, A study of the effects of filler particles on the degradation mechanisms of powder epoxy novolac coating systems under corrosion and erosion, Prog. Org. Coat. 121 (2018) 97–104. https://doi.org/10.1016/j.porgcoat.2018.04.026.

20. M. Fernández-Álvarez, F. Velasco, A. Bautista, Effect on wear resistance of nanoparticles addition to a powder polyester coating through ball milling, J. Coat. Tecnhol. Res. 15 (2018) 771–779. https://doi.org/10.1007/s11998-018-0106-z.

21. D. Stkhlberg, M. Johansson, Properties of powder coatings in load carrying construction, J. Coat. Tecnhol. Res. 2 (2005) 473–481. https://doi.org/10.1007/BF02733890.

22. P. Jawahar, R. Gnanamoorthy, M. Balasubramanian, Tribological behaviour of clay - thermoset polyester nanocomposites, Wear 261 (2006) 835–840. https://doi.org/10.1016/j.wear.2006.01.010

23. D. Piazza, A.F. Baldissera, S.R. Kunst, E.S. Rieder, L.C. Scienza, C.A. Ferreira, A.J. Zattera, Influence of the addition of montmorillonite in an epoxy powder coating applied on carbon steel, Mater. Res. 18 (2015) 897–903. https://doi.org/10.1590/1516-1439.312714.

24. G.A.S. Catarina, C. Borsoi, D. Romanzini, D. Piazza, S.R. Kunst, L.C. Scienza, A.J. Zattera, Development of acrylic-based powder coatings with incorporation of montmorillonite clays, J. Appl. Polym. Sci. 134 (2017) 45031. https://doi.org/10.1002/app.45031.

25. Q. Shi, W. Huang, Y. Zhang, Y. Zhang, Y. Xu, G. Guo, Curing of polyester powder coating modified with rutile nano-sized titanium dioxide studied by DSC and real-time FT-IR, J. Therm. Anal. Calorim. 108 (2012) 1243–1249. https://doi.org/10.1007/s10973-011-1855-4.

26. Evonik, AEROSIL® - fumed silica Technical overview, Available at https://www.aerosil.com/sites/lists/RE/DocumentsSI/Technical-Overview-AEROSIL-FumedSilica-EN.pdf. (accessed on October 2nd, 2019)

27. M.M. Jalili, S. Moradian, H. Dastmalchian, A. Karbasi, Investigating the variations in properties of 2-pack polyurethane clear coat through separate incorporation of hydrophilic and hydrophobic nano-silica, Prog. Org. Coat. 59 (2007) 81–87. , https://doi.org/10.1016/j.porgcoat.2007.01.018.

28. X. Shi, T.A. Nguyen, Z. Suo, Y. Liu, R. Avci, Effect of nanoparticles on the anticorrosion and mechanical properties of epoxy coating, Surf. Coat. Technol. 204 (2009) 237–245. https://doi.org/10.1016/j.surfcoat.2009.06.048.

29. D.K. Owens, R.C. Wendt, Estimation of the surface free energy of polymers, J. Appl. Polym. Sci. 13 (1969) 1741–1747, https://doi.org/10.1002/app.1969. 070130815.

30. D.H. Kaelble, Dispersion-polar surface tension properties of organic solids, J. Adhes. 2 (1970) 66–81. https://doi.org/10.1080/0021846708544582.

31. H.E. Kissinger, Reaction kinetics in differential Thermal Analysis, Anal. Chem. 29 (1957) 1702–1706, https://doi.org/10.1021/ac60131a045.

32. S. Vyazovkin, C.A. Wight, Model-free and model-fitting approaches to kinetic analysis of isothermal and nonisothermal data, Thermochim. Acta. 340–341 (2002) 53–68. https://doi.org/10.1016/S0040-6031(99)00253-1.

33. D. Lascano, L. Quiles-Carrillo, R. Balart, T. Boronat, N. Montanes, Kinetic analysis of the curing of a partially biobased epoxy resin using dynamic differential scanning calorimetry, Polymers 11 (2019). https://doi.org/10.3390/polym11030391.

34. J.M. Durand, M. Vardavoulias, M. Jeandin, Role of reinforcing ceramic particles in the wear behaviour of polymer-based model composites, Wear 181–183 (1995) 833–839. https://doi.org/10.1016/0043-1648(95)90203-1.

35. J. Abenojar, J. Tutor, Y. Ballesteros, J.C. del Real, M.A. Martínez, Erosion-wear, mechanical and thermal properties of silica filled epoxy nanocomposites, Compos. Part B Eng. 120 (2017) 42–53. https://doi.org/10.1016/j.compositesb.2017.03.047.

36. Q.B. Guo, M.Z. Rong, G.L. Jia, K.T. Lau, M.Q. Zhang, Sliding wear performance of nano-SiO_2/short carbon fiber/epoxy hybrid composites, Wear 266 (2009) 658–665. https://doi.org/10.1016/j.wear.2008.08.005.

37. J. Zhang, L. Chang, S. Deng, L.Ye, Z. Zhang, Some insights into effects of nanoparticles on sliding wear performance of epoxy nanocomposites, Wear 304 (2013) 138–143. https://doi.org/10.1016/j.wear.2013.04.037.

38. A. Allahverdi, M. Ehsani, H. Janpour, S. Ahmadi, The effect of nanosilica on mechanical, thermal and morphological properties of epoxy coating, Prog. Org. Coat. 75 (2012) 543–548. https://doi.org/10.1016/j.porgcoat.2012.05.013.

39. M. Hedayati, M. Salehi, R. Bagheri, M. Panjepour, F. Naeimi, Tribological and mechanical properties of amorphous and semi-crystalline PEEK/SiO_2 nanocomposite coatings deposited on the plain carbon steel by electrostatic powder spray technique, Prog. Org. Coat. 74 (2011) 50–58. https://doi.org/10.1016/j.porgcoat.2011.09.014.

40. M. Malaki, Y. Hashemzadeh, M. Karevan, Effect of nano-silica on the mechanical properties of acrylic polyurethane coatings, Prog. Org. Coat. 101 (2016) 477–485. https://doi.org/10.1016/j.porgcoat.2016.09.012

41. C.L. Wu, M.Q. Zhang, M.S. Rong, K. Friedrich, Tensile performance improvement of low nanoparticles filled-polypropylene composites, Compos. Sci. Techn. 62 (2002) 1327–1340. https://doi.org/10.1016/S0266-3538(02)00079-9.

42. N.K. Myshkin, M.I. Petrokovets, A. V. Kovalev, Tribology of polymers: Adhesion, friction, wear, and mass-transfer, Tribol. Int. 38 (2005) 910–921. https://doi.org/10.1016/j.triboint.2005.07.016.

43. M. Jouyandeh, O.M. Jazani, A.H. Navarchian, M. Shabanian, H. Vahabi, M.R. Saeb, Surface engineering of nanoparticles with macromolecules for epoxy curing: Development of super-reactive nitrogen-rich nanosilica through surface chemistry manipulation, Appl. Surf. Sci. 447 (2018) 152–164. https://doi.org/10.1016/j.apsusc.2018.03.197

44. R. Mafi, S.M. Mirabedini, M.M. Attar, S. Moradian, Cure characterization of epoxy and polyester clear powder coatings using Differential Scanning Calorimetry (DSC) and

Dynamic Mechanical Thermal Analysis (DMTA), Prog. Org. Coat. 54 (2005) 164–169. https://doi.org/10.1016/j.porgcoat.2005.06.006.

45. E.G. Belder, H.J.J. Rutten, D.Y. Perera, Cure characterization of powder coatings, Prog. Org. Coat. 42 (2001) 142–149. https://doi.org/10.1016/S0300-9440(01)00149-7.

46. R. Mafi, S.M. Mirabedini, R. Naderi, M.M. Attar, Effect of curing characterization on the corrosion performance of polyester and polyester/epoxy powder coatings, Corros. Sci. 50 (2008) 3280–3286. https://doi.org/10.1016/j.corsci.2008.08.037.

47. L. Halász, K. Belina, An investigation into the curing of epoxy powder coating systems, J. Therm. Anal. Calorim. 119 (2015) 1971–1980. https://doi.org/10.1007/s10973-015-4411-9.

48. N. Causse, E. Dantras, C. Tonon, M. Chevalier, H. Combes, P. Guigue, C. Lacabanne, Enthalpy relaxation phenomena of epoxy adhesive in operational configuration: Thermal, mechanical and dielectric analyses, J. Non. Cryst. Solids. 387 (2014) 57–61. https://doi.org/10.1016/j.jnoncrysol.2013.12.028.

49. M.A. Safarpour, A. Omrani, S. Afsar, D. Zare-Hossein-Abadi, Study of cure kinetics of epoxy/DDS/nanosized (SiO_2/TiO_2) system by dynamic differential scanning calorimetry, Polym. Adv. Technol. 22 (2011) 718–723. https://doi.org/10.1002/pat.1571.

50. A.Q. Barbosa, L.F.M. Da Silva, J. Abenojar, J.C. Del Real, R.M.M. Paiva, A. Öchsner, Kinetic analysis and characterization of an epoxy/cork adhesive, Thermochim. Acta. 604 (2015) 52–60. https://doi.org/10.1016/j.tca.2015.01.025.

51. M. Fernández-Álvarez, F. Velasco, A. Bautista, J. Abenojar, Effect of silica nanoparticles on the curing kinetics and erosion wear of an epoxy powder coating, J. Mater. Res. Technol. (2019). https://doi.org/10.1016/j.jmrt.2019.10.073.

52. D.E. Lee, H.W. Kim, B. Kong, H.O. Choi, A study on the curing kinetics of epoxy molding compounds with various latent catalysts using differential scanning calorimetry, J. Appl. Polym. Sci 134 (2017) 45252. https://doi.org/10.1002/app.45252.

53. A. Burkanudeen, P. Ramesh, Novel latent epoxy curing agent for secondary insulation in electrical rotors and stators, IEEE Trans. Dielectr. Electr. Insul. 19 (2012) 1791–1798. https://doi.org/10.1109/TDEI.2012.6311529.

54. M. Ghaffari, M. Ehsani, H.A. Khonakdar, G. Van Assche, H. Terryn, The kinetic analysis of isothermal curing reaction of an epoxy resin-glassflake nanocomposite, Thermochim. Acta. 549 (2012) 81–86. https://doi.org/10.1016/j.tca.2012.09.021.

55. M. Nonahal, M.R. Saeb, S. Hassan Jafari, H. Rastin, H.A. Khonakdar, F. Najafi, F. Simon, Design, preparation, and characterization of fast cure epoxy/amine-functionalized graphene oxide nanocomposites, Polym. Compos. 39 (2018) E2016–E2027. https://doi.org/10.1002/pc.24415.